Current Nanoscience, 2018, *14*, 234-238

RESEARCH ARTICLE

Influences of Morphology of Window Layer on the Characteristics of PbS Quantum Dot Solar Cells

Nguyen Thu Ha and Nguyen Dinh Lam*

Department of Physics, Hanoi National University of Education, 136, Xuanthuy, Caugiay, Hanoi, Vietnam

ARTICLE HISTORY

Received: August 29, 2017
Revised: January 09, 2018
Accepted: January 29, 2018

DOI:
10.2174/1573413714666180201162746

Abstract: ***Background***: In QDs-based solar cell devices, the PbS QDs layer was mainly focused to optimize. The ZnO electron acceptor layer attracts less attention whereas it shows the key roles in extracting and transporting charge carriers in heterojunction. The utilization of 1-D ZnO structures has been demonstrated to be large interface areas and good carrier pathways for efficient carrier collection. However, the influences of the morphology of metal oxide nanostructures on the photovoltaic performance of QD-based solar cells have been few in-depth reports.

Objective: In this work, ZnO NRs/PbS QD based solar cells were fabricated. The influences of the ZnO NRs array structures on characteristics of ZnO NRs/PbS QD based solar cells were investigated.

Method: ZnO NRs/PbS QD based solar cells were fabricated via spin coating method. XRD, SEM, UV-VIS-NIR spectrophotometer, I-V and EQE measurement systems were utilized to investigate the fabricated samples.

Results: We have found optimum combinations of the linked parameters of ZnO NRs, their length of (230 ± 5) nm and density of (1.50 ± 5)x10^{10} # of rods.cm^{-2}, that exhibit maximum efficiency of ~2.5% for the ZnO NR/PbS QDs based solar cell.

Conclusion: The influences the ZnO NRs structures on the solar cell characteristics, including the absorption, external quantum efficiency, and current density-voltage curves, were investigated. There seems to be an optimum between NR length and their density for resulting in maximum efficiency. This could be due the interplay of solar flux absorption and junction area controlled by these two parameters of ZnO NR morphology.

Keywords: ZnO nanorod, nanorod length, nanorod density, PbS quantum dot, solar cell, window layer.

1. INTRODUCTION

In recent years, quantum dots (QDs) have been widely utilized for solar cell (SC) device fabrication because of their size-dependent band-gap tenability [1-5]. A variety of QDs-based solar cell structures have been designed [4-8]. The most common QDs-based solar cell structure is formed based on the combination of a low band-gap semiconductor QDs and wide-band-gap metal oxide semiconductor [4, 6, 7]. In this structure, QDs work as light absorber layer and hole conductor and metal oxide work as an electron acceptor and conductor. For the absorption of infrared light in solar spectrum, PbS QDs have been widely utilized to fabricated QDs-based solar cell devices [4, 7-9]. Based on the high electron mobility, low cost of production, abundance in nature, chemically stable crystal structure and high transparency characteristics of zinc oxide (ZnO), it has been widely used as an electron acceptor and conductor material [4, 5].

In QDs-based solar cell devices, the PbS QDs layer was mainly focused to optimize. The ZnO electron acceptor layer attracts less attention whereas it shows the key roles in extracting and transporting charge carriers in heterojunction. By optimizing the ZnO electron acceptor layer, a power conversion efficiency rising up to 6.7% has been obtained with an optimized thickness of 90 nm [9, 10]. Furthermore, different 1-D ZnO structures such as nanowires (NWs), nanorods (NRs), and nanotubes (NTs), have been fabricated for organic, dye-sensitized [11] and thin film solar cells [6, 12-17]. The utilization of 1-D ZnO structures has been demonstrated to be large interface areas and good carrier pathways for efficient carrier collection. However, the influences of the morphology of metal oxide nanostructures on the photovoltaic performance of QD-based solar cells have been few

*Address correspondence to this author at the Department of Physics, Hanoi National University of Education, 136, Xuanthuy, Caugiay, Hanoi, Vietnam; Tel: +84 902 233 144; E-mail: lam.nd@hnue.edu.vn

1875-6786/18 $58.00+.00

in-depth reports. In this work, ZnO NRs/PbS QD based solar cells were fabricated. The influences of the ZnO NRs array structures on characteristics of ZnO NRs/PbS QD based solar cells were investigated.

2. MATERIALS AND METHOD

ZnO NRs/PbS QD based solar cells were designed by combining PbS QDs with ZnO NR arrays. The first absorption peak of PbS QD was at the wavelength of 1200 nm (PbS QD size is about 5.5nm). ZnO NR arrays with different structures were grown on ITO-coated glass substrates with a ZnO seed layer by a hydrothermal method. The hydrothermal temperatures were varied from 70 to 90^{o}C in order to change the structures of ZnO NR arrays. During hydrothermal process, the growth time, concentration and volume of solution were kept as constants. The PbS QD layer was deposited on the ZnO NR array from a PbS QD octane solution (20mg.mL^{-1}) using the layer-by-layer spin-coating method. The deposited PbS QD layers were treated with a 1,3-benzenedithiol (BDT) solution in acetonitrile to replace the native oleic acid capping ligands. After ligands exchange process, the substrate was rinsed three times with acetonitrile to remove excess ligands and spun dry. The PbS QD coating process was repeated 3 times to get the total PbS QD layer thickness of ~420 nm. Finally, a 100 nm Au back contact layer was then thermally evaporated through a shadow mask. The active device area of 1.5 cm^{2} is defined by the overlap of the Au anode with the ITO cathode.

X-ray diffraction pattern of the ZnO NR array was measured by an X-Ray Diffractometer (XRD) D5000 with CuKα radiation (λ = 1.5406 Å) at room temperature. The morphology of ZnO NRs arrays and ZnO NRs/PbS QD solar cells were investigated using a Scanning Electron Microscope (SEM). The density and length of ZnO NRs were determined from SEM images. The optical spectra of ZnO NR arrays and ZnO NRs/PbS QD solar cell were studied using a UV–VIS-NIR (V670) spectrophotometer at room temperature. The photovoltaic current density-voltage (J-V) characteristics of ZnO NRs/PbS QD solar cell are determined by a solar simulator under 1 sun air mass 1.5G at room temperature. The photocurrent response of the fabricated cells was also investigated at room temperature using a quantum efficiency measurement system.

3. RESULTS AND DISCUSSION

Top- and side-view SEM images of ZnO NR structures at different growth temperature are shown in Fig. (**1**). The ZnO NR structures are denoted as #1 (70^{o}C), #2 (80^{o}C), and #3 (90^{o}C). The images show that ZnO NRs are of uniform size and have a tendency to become oriented perpendicular to the surface of the substrates. Moreover, the length and density of ZnO NR structures strongly depend on the growth temperature. These dependences were extracted and depicted in Fig. (**2**). This result indicated that density and length of the ZnO NR increase with an increasing of the growth temperature. The longest of rod length of (270±5) nm is obtained when the growth temperature is 90^{o}C. However, the density of the ZnO NR can reach to a maximum value when the growth temperature is 80^{o}C.

Fig. (**3a**) shows the X-ray diffraction (XRD) pattern of the ZnO NRs grown at 80^{o}C. The XRD pattern indicates that the structure of the ZnO NR is polycrystalline. The presence of the (100), (002), (101), (102), (110), and (103) peaks in the XRD pattern also indicates hexagonal wurtzite structure of ZnO. Diffraction peaks related to no other phases are observed in the XRD patterns. Furthermore, the high c-axis oriented (002) of the ZnO NR may be good for enhancement the mobility of charge carriers [18]. The influences of the different ZnO NR structures on optical transmittance is shown in Fig. (**3b**). The optical transmittance depends on ZnO structure and to be strongly reduced in visible region when the length of ZnO NR increases. Thus, higher absorption of visible light can be correlated with higher generation of charge carriers.

Fig. (**4**) shows the surface and cross-section (inset) SEM images of the ZnO NRs/PbS QD after the PbS QDs coating process. The PbS QDs layer was deposited via layer by layer spin coating. Due to the spin coating method, it can be clearly observed some small part incomplete QDs infiltration on the surface and in the ZnO NR structure. Furthermore, based on the rod length and rod density of the ZnO NR structures,

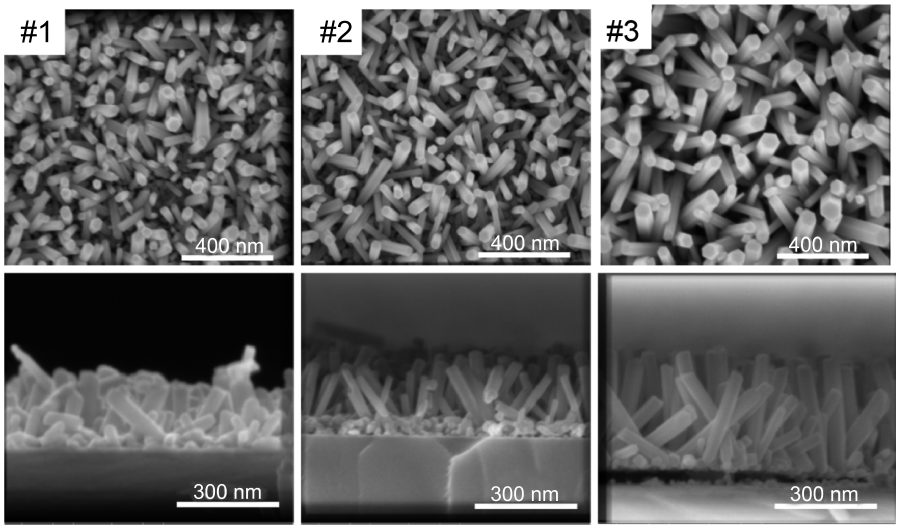

Fig. (1). Top- and side-view SEM images of ZnO NR structures at different growth temperature #1 (70^{o}C), #2 (80^{o}C), and #3 (90^{o}C).

the effective surface areas were calculated from the total surface areas of NRs. The calculated effective surface area of #1, #2, and #3 ZnO NR structure is 2.1, 4.7, and 4.1 cm^2, respectively. This result indicated that the depletion area of #1, #2, and #3 ZnO NR structure could be enhanced up to 2.1, 4.7, and 4.1 times compared to that of a ZnO film.

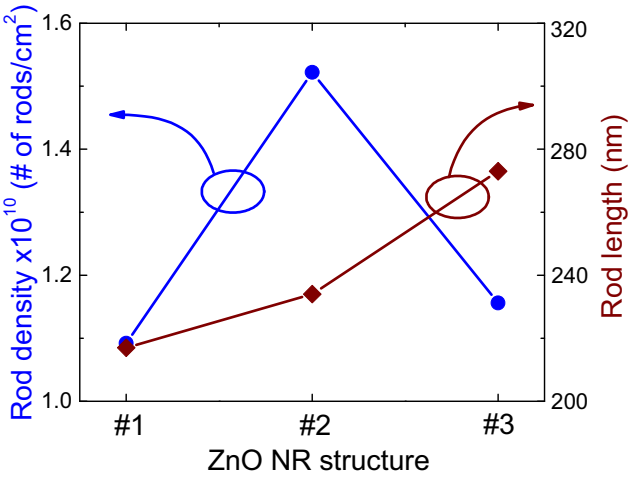

Fig. (2). The length, and density of ZnO NR structures with different growth temperature.

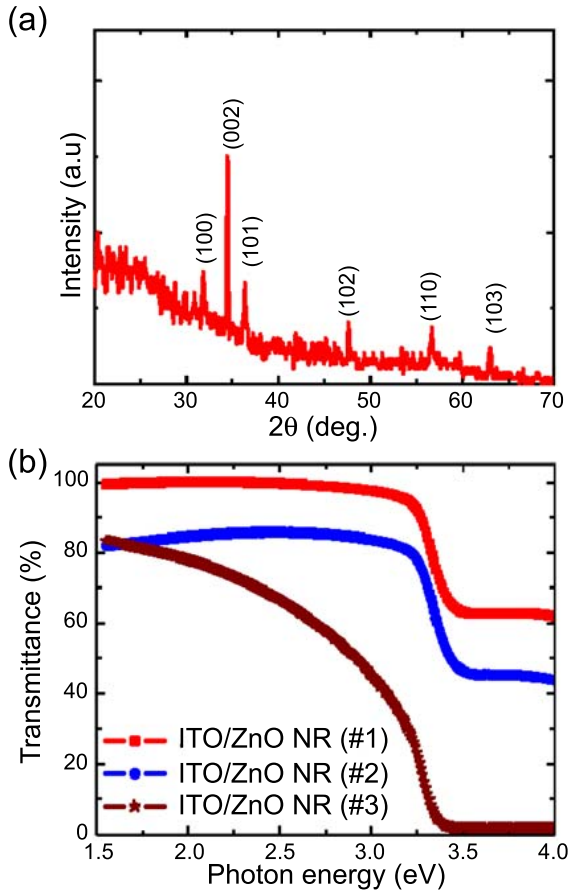

Fig. (3). (**a**) X-ray diffraction (XRD) pattern of the ZnO NRs grown at 80°C. (**b**) Optical transmittance of ZnO NR structures with different growth temperature.

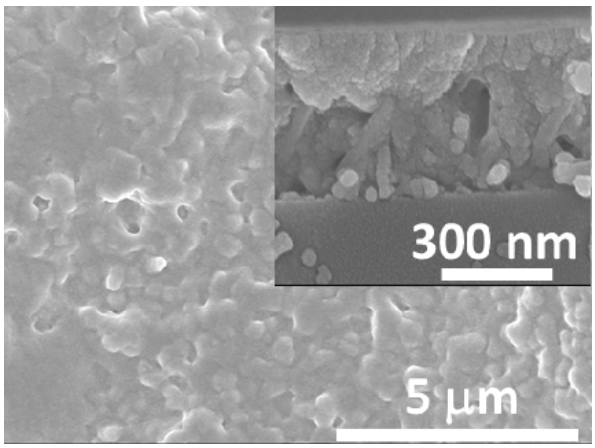

Fig. (4). The surface and cross-section (inset) SEM images of the ZnO NRs/PbS QDs after the PbS QDs coating process.

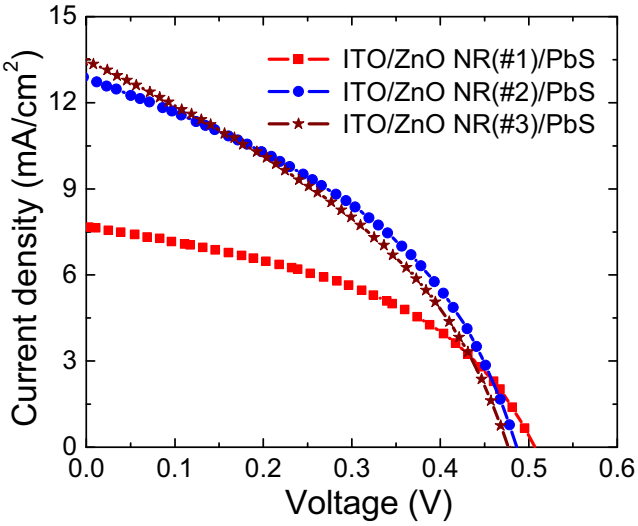

Fig. (5). The J–V characteristics of ZnO NR/PbS QD solar cells depended on density and length of ZnO NRs.

The J–V characteristics of ZnO NR/PbS QD solar cells depend on density and length of ZnO NRs as shown in Fig. (**5**). The highest Voc of 0.51V and Jsc of 13.38 mA/cm^2 was obtained with ZnO NR(#1)/PbS and ZnO NR(#3)/PbS, respectively. For more detail analysis, the short-circuit current density (Jsc), open-circuit voltage (Voc), fill factor (FF) and power conversion efficiency (PCE) obtained for the solar cells were extracted and replotted as a function of the length and density of the ZnO NRs in Figs. (**6a**) and (**6b**), respectively. In Fig. (**6a**), the results show that the Jsc increases with an increasing of the length of the ZnO NRs. This improvement of the Jsc may be attributed to the enhanced photocarrier generation in case of longer ZnO NRs and their probable improved collection. The Voc and FF are slightly reduced when the length of ZnO NRs increases. These reductions could be attributed to inability of QDs to reach deeper in the NR mesh during the spin coating process, and thus reducing the effective junction area. This is also verified by the value of the shunt resistance (Rsh) and series resistance

(Rs). The samples #2 and #3 both showed near maximum solar cell parameters in the present study, larger than the sample #1. This could be attributed to higher absorption in more dense NRs and due to larger effective junction area in longer NRs.

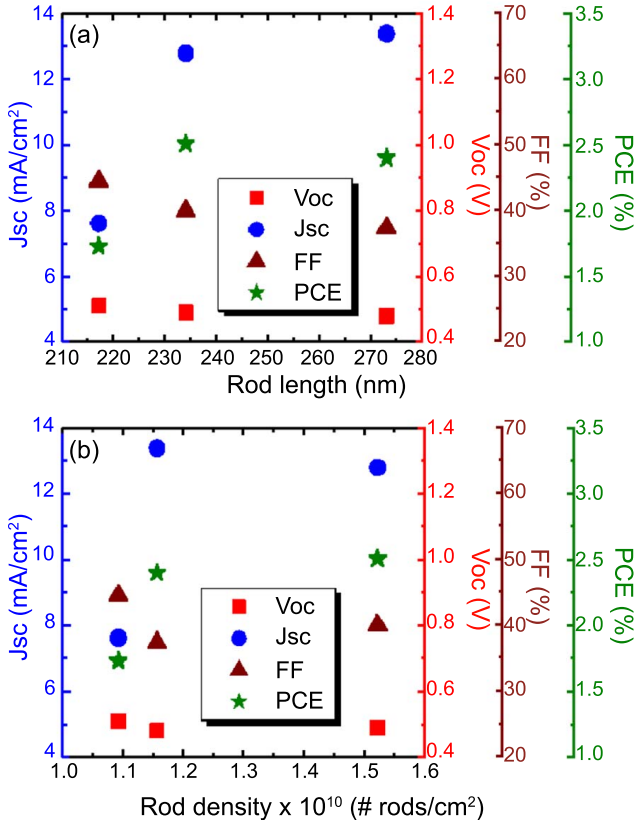

Fig. (6). Solar cell performances for ZnO NR/PbS QD solar cells fabricated with different ZnO NR (**a**) lengths and (**b**) densities.

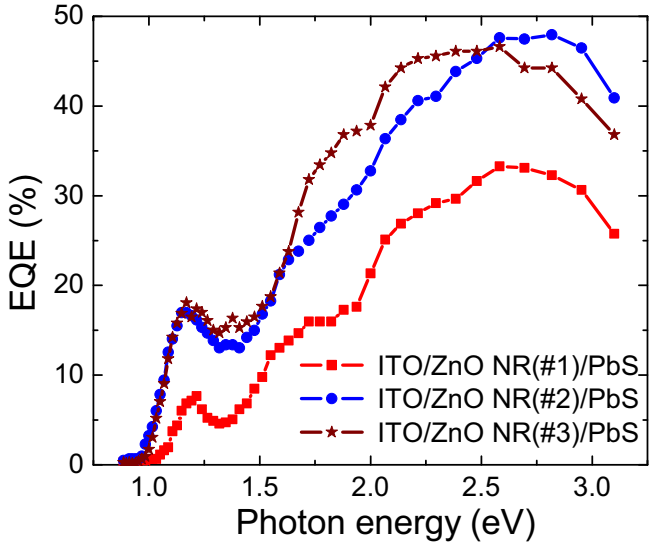

Fig. (7). External quantum efficiency (EQE) of the ZnO NRs/PbS QDs solar cells.

The external quantum efficiency (EQE) of the three types of the ZnO NRs/PbS QD based devices was measured and is shown in Fig. (**7**). The solar cell with the ZnO NRs (#1) gave an EQE of 7.8% at the low energy absorption peak observed at 1.2 eV. The value of EQE was improved with the ZnO NRs (#2 and #3) and reached to a maximum value of 18.5% in the solar cell with the ZnO NRs (#3). Accordingly, Jsc increased with longer ZnO NRs length and reached to a maximum value of 13.38 $mAcm^{-2}$ with the ZnO NRs (#3). This maximum value is approximately twice the value obtained for the ZnO NRs (#1) (7.62 $mAcm^{-2}$). This result demonstrates that the longer ZnO NRs length could more efficiently extract charge carriers from PbS QD layers [6].

CONCLUSION

In this work, the role of the ZnO NRs structure in ZnO NR/PbS QDs based solar cells was demonstrated. The influences the ZnO NRs structures on the solar cell characteristics, including the absorption, external quantum efficiency, and current density-voltage curves, were investigated. There seems to be an optimum between NR length and their density for resulting in maximum efficiency. This could be due the interplay of solar flux absorption and junction area controlled by these two parameters of ZnO NR morphology

ETHICS APPROVAL AND CONSENT TO PARTICIPATE

Not applicable.

HUMAN AND ANIMAL RIGHTS

No Animals/Humans were used for studies that are base of this research.

CONSENT FOR PUBLICATION

Not applicable.

CONFLICT OF INTEREST

The authors declare no conflict of interest, financial or otherwise.

ACKNOWLEDGEMENTS

This research is funded by Vietnam National Foundation for Science and Technology Development (NAFOSTED) under grant number 103.99-2014.60.

REFERENCES

[1] Tian, J.; Shen, T.; Liu, X.; Fei, C; Lv, L.; Cao, G. Enhanced performance of PbS-quantum-dot-sensitized solar cells *via* optimizing precursor solution and electrolytes. *Sci. Rep.*, **2016**, *6*, 23094.

[2] Zheng, Z.; Ji, H.; Yu, P.; Wang, Z. Recent progress towards quantum dot solar cells with enhanced optical absorption. *Nanoscale Res. Lett.*, **2016**, *11*, 266.

[3] Wang, H.; Victoria, G.P.; Takaya, K.; Francisco, F.S.; Juan, B.; Yoshitaka, S.; Nakazaki, J.; Segawa, H. Enhanced carrier transport distance in colloidal PbS quantum-dot-based solar cells using ZnO nanowires. *J. Phys. Chem. C*, **2015**, *119*(49), 27265-27274.

[4] Chia-Hao, M.C.; Patrick, R.B.; Bulović, V.; Moungi, G.B. Improved performance and stability in quantum dot solar cells

through band alignment engineering. *Nat. Mater.,* **2014**, *13*, 796-801.

[5] Sawsan, D.; Haik, Y.; Tit, N.; Ayesh, A. PbS/CdS heterojunction quantum dot solar cells. *J. Mater. Sci. Mater. Electron*., **2016**, *27*(4), 3328-3340.

[6] Jean, J.; Chang, S.; Brown, P.R.; Cheng, J.J.; Rekemeyer, P.H.; Bawendi, M.G.; Gradecak, S.; Bulovic, V. ZnO Nanowire arrays for enhanced photocurrent in PbS quantum dot solar cells. *Adv. Mater.,* **2013**, *25*, 2790-2796.

[7] Gao, J.; Luther, J.M.; Semonin, O.E.; Rllingson, R.J.; Nozik, A.J.; Beard, M.C. Quantum dot size dependent J−V characteristics in heterojunction ZnO/PbS quantum dot solar cells. *Nano Lett*., **2011**, *11*, 1002-1008.

[8] Yoon, W.; Boercker, J.E.; Lumb, M.P.; Placencia, D.; Foos, E.E.; Tischler, J.G. Enhanced open-circuit voltage of PbS nanocrystal quantum dot solar cells. *Sci. Rep*., **2013**, *3*, 2225.

[9] Kumar, D.; Bai, R; Chaudhary, S.; Pandya, D.K. Enhanced photoelectrochemical response for hydrogen generation in self-assembled aligned ZnO/PbS core/shell nanorod arrays grown by chemical bath deposition. *Mater. Today Energy*, **2017**, *6*, 105-114.

[10] Yang, X.; Hu, L.; Deng, H.; Qiao, K.; Hu, C.; Liu, Z.; Yuan, S.; Kha, J.; Li, D.; Tang, J.; Song, H.; Cheng, C. Improving the performance of PbS quantum dot solar cells by optimizing ZnO window layer. *Nano-Micro Lett.,* **2017**, *9*, 24.

[11] Singh, T.; Pandya, D.K.; Singh, R. Concentration dependent structural and optical properties of electrochemically grown ZnO thin films and nanostructures. *Appl. Surf. Sci.*, **2013**, *270*, 578-583.

[12] Kawawaki, T.; Wang, H.; Kubo, T.; Saito, K.; Nakazaki, J.; Segawa, H.; Tatsuma, T. Efficiency enhancement of PbS quantum dot/ZnO nanowire bulk-heterojunction solar cells by plasmonic silver nanocubes. *ACS Nano*, **2015**, *9*(4), 4165-4172.

[13] Ko, S.H.; Lee, D.; Kang, H.W.; Nam, K.H.; Yeo, J.Y.; Hong, S.J.; Grigoropoulos, C.P.; Sung, H.J. Nanoforest of hydrothermally grown hierarchical ZnO Nanowires for a high efficiency dye-sensitized solar cell. *Nano Lett.*, **2011**, *11*, 666-671.

[14] Nayeri, F.D.; Akbarnejad, E.; Ghoranneviss, M.; Soleimani, E.A.; Hashemizadeh, S.A. Dye decorated ZnO-NWs /CdS-NPs heterostructures for efficiency improvement of quantum dots sensitized solar cell. *Superlattices Microstruct.,* **2016**, *91*, 244-251.

[15] Tian, J.; Zhang, Q.; Uchaker, E.; Liang, Z.; Gao, R.; Qu, X.; Zhang, S.; Cao, G. Constructing ZnO nanorod array photoelectrodes for highly efficient quantum dot sensitized solar cells. *J. Mater. Chem. A*, **2013**, *1*, 6770-6775.

[16] Valls, I.G.; Yu, Y.; Ballesteros, B.; Oro, J.; Cantu, M.L. Synthesis conditions, light intensity and temperature effect on the performance of ZnO nanorods-based dye sensitized solar cells. *J. Power Sources*, **2011**, *196*, 6609-6621.

[17] Han, J.; Fan, F.; Xu, C.; Lin, S.; Wei, M.; Duan, X.; Wang, Z.L. ZnO nanotube-based dye-sensitized solar cell and its application in self-powered devices. *Nanotechnology*, **2010**, *21*, 405203.

[18] Sun, Y.; Seo, J.H.; Takacs, C.J.; Seifter, J.; Heeger, A.J. Inverted polymer solar cells integrated with a low-temperature-annealed sol-gel-derived ZnO film as an electron transport layer. *Adv. Mater*., **2011**, *23*, 1679-1683.